EVALUATION OF TWO REGION BASED CLASSIFICATIONS IN TAPAJÓS NATIONAL FOREST USING THE ALOS/PALSAR POLARIMETRIC AND INTERFEROMETRIC COHERENCES

Graziela Balda Scofield[1], Luciano Vieira Dutra[1], Corina da Costa Freitas[1], Sidnei João Siqueira Sant´Anna[1], Daniel Luis Andrade Silva[2]

[1]Instituto Nacional de Pesquisas Espaciais - INPE
Caixa Postal 515 - 12245-970 - São José dos Campos - SP, Brasil
{graziela, dutra, corina, sidnei@dpi.inpe.br}

[2]Diretoria de Serviço Geográfico - DSG
Quartel General do Exército - Bloco "F" - SMU - 70630-901 - Brasília - DF, Brasil
cartografoniel@yahoo.com.br

1. INTRODUCTION

The land cover classification is one of the principal objectives of the remote sensing data analysis. The use of single-polarization data (HH, HV or VV) is limited to separate different targets providing a low accuracy in the land cover classification results. Several studies have been showed that the use of phase information presents in complex multi polarized images may increase the classification results. The coherence is one attribute that might be extracted from these images and it may be used to discriminate some land cover classes. The class discrimination is achieved, since low coherence values are normally observed on primary, secondary forests and reforestations while high coherence values are characteristics of pasture, agricultures and bare soil. On the other hand, region classifiers have widely been applied for mapping different land cover classes. Therefore, the use of region classification approach with coherence information seems to be helpful for the mapping task, as already demonstrated in [1] and [2]. The aim of this work is to evaluate region classification results of two different segmentation algorithms: the SegSAR [3] and the region growing algorithm presented in SPRING software [4]. In order to conduct the evaluation, several multi-band images were generated. In order to conduct the evaluation, several multi-band images were generated. A multi-band image is composed by one coherence and two intensity channels. Finally, these images were segmented and after they were classified using the Bhattacharyya distance. The classifications were quantified by the overall accuracy, the kappa values and its variance.

2. MATERIALS AND METHODS

2.1. Materials

Two full polarimetric (PLR) scenes from ALOS/PALSAR acquired on March 8th and April 23rd, 2007 over Tapajós National Forest in the Brazilian Amazon were used on the evaluation process. The two intensities

channels of every multi-band image are derived from the polarimetric bands of the scene taken on April 23. This scene was also used to extract the polarimetric coherence between the HH and VV bands, called by HH_VV. According to [5], the HH and VV bands present stronger backscatter than the cross-polarizations. The former scene was only used to generate two interferometric coherences. The interferometric coherences are based on HH and HV bands of the two radar scenes and are denominated HH1_HH2 and HV1_HV2, respectively. The VV1_VV2 image was not used due to processing problems.

2.2 Methods

The flow chart in Fig. 1 summarizes all the steps for the applied region classifications. First, the interferometric and polarimetric coherence images are calculated using two complex images of the polarimetric or interferometric pair, as defined by equation (1),

$$\hat{\gamma} = \frac{\left\langle p_1 p_2^{*} \right\rangle}{\sqrt{\left\langle |p_1|^2 \right\rangle \left\langle |p_2|^2 \right\rangle}} \tag{1}$$

where $\langle . \rangle$ is a spatial averaging operator of the signal complex compounds, p_1 e p_2 are, respectively, the complex pixels of images 1 and 2 belonging to the polarimetric or interferometric pair and $|\hat{\gamma}|$ is the estimation of the polarimetric and interferometric coherences, whose value is between 0 and 1.

The obtained coherence images depend on a precise complex image co-register with sub-pixel order. After the complex image co-register, a n x m boxcar filter should be used to estimate the complex correlation coefficient.

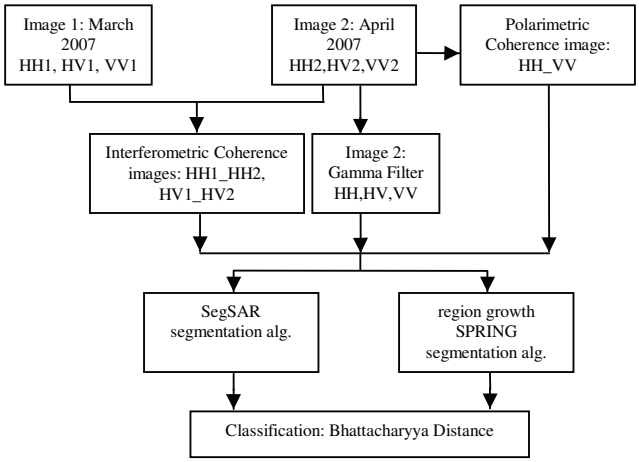

Fig. 1: Flow chart of the activities

For the intensity multi-polarimetric images taken on April 23, the standard Gamma speckle filtering method (5x5 window) was applied. With the interferometric and polarimetric coherence and muti-polarimetric filtered images, nine sets with three images (two polarimetric and one polarimetric or interferometric

coherence channels) and three sets with two intensity images were segmented in each segmentation algorithm and finally classified. The two segmentation strategies applied were the SegSAR (SS) and the region-growing SPRING (SP) segmentation algorithms. The SegSAR algorithm uses region growing, split and merge techniques and edge adjustment and it was developed considering the statistical properties of SAR and optical data. The region growing SPRING segmentation occurs if two neighbor regions are similar (mean test), if the similarity satisfies the threshold, and if two regions are mutually near. After the segmentation phase, the Bhattacharyya Distance (BD), which is a measure of statistical distance between probability density functions is used, as an association criterion between the region with unknown label and one of the training classes. It is assumed that all studied regions and classes are normally distributed. Henceforth, the classification results will be represented by SS for SegSAR and SP for SPRING.

3. RESULTS AND CONCLUSIONS

The performance of the SS and SP classifications are quantified in Table 1 by the overall accuracy, $\hat{\kappa}$ values and its variances. The results are presented in descending order of SS overall accuracy and the SS and SP results are showed for each multi-band image. In Fig. 2 is shown the color composition image HV(R), VV(G), HV1_HV2 (B) with the class training samples locations, its segmentation and its classification using SS. This set presented the best overall accuracy and kappa values.

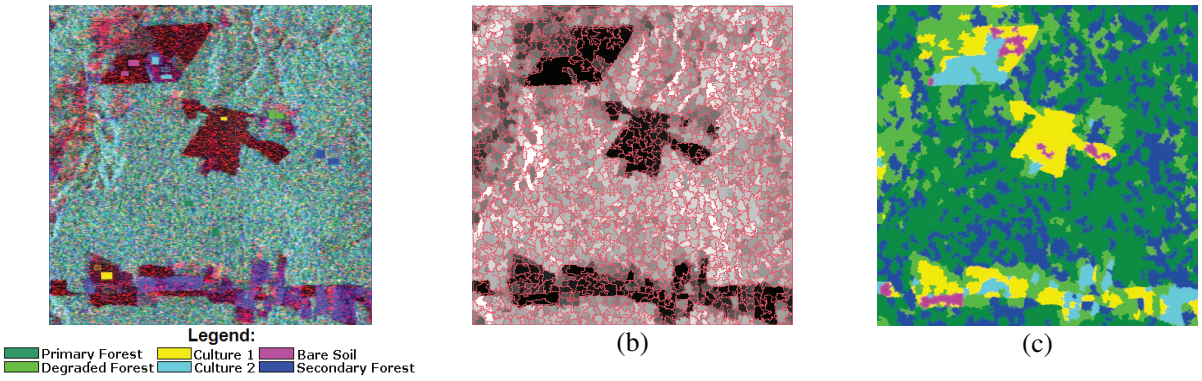

(a) (b) (c)

Fig. 2. (a) (HV)R, (VV)G, (HV1_HV2)B color composition, (b) its segmentation and (c) its classification images using SS.

The statistical tests evaluate the equality between each pair of $\hat{\kappa}$ values. The tests of equality of $\hat{\kappa}$ demonstrated that most classifications may be considered different from each other at a significance level of 5%. However, there was no statistical evidence of differences between the $\hat{\kappa}$ value pairs of the classifications: (SS-HH, VV, HV1_HV2 and SS-HH, HV, HH_VV); (SS-HH, HV, HV1_HV2 and SS-HV, VV, HH1_HH2); (SS-HH, HV, HV1_HV2 and SP-HV, VV, HH_VV); and (SS-HH, HV, HV1_HV2 and SP-HH, VV, HH1_HH2). Analyzing all multi-band images with HH1_HH2 data, the best overall accuracy values are obtained using the SP for all cases, although the pairs of SS-HV, VV, HH1_HH2 and SP-HH, VV and HH1_HH2 may not be considered different from each other at a significance level of 5%. The multi-band images with HV1_HV2 channel presented the best overall accuracies for the SS segmentation algorithm. The

multi-band images with HH_VVchannel showed the best performance using SS, even though the pairs of SS-HV, VV, HH_VV and SP-HH, VV, HH_VV; and SS-HH, VV, HH_VV and SP-HH, HV, HH_VV presented no statistical evidence of differences between the $\hat{\kappa}$ values at a significance level of 5%. Examining the two band classification results, the HH, VV set presented the lowest accuracy values while the best two band result was for HH, HV. Even though the best two band classification were done with HH and HV bands , the best classifications were with the SS-HV, VV, HV1_HV2 and SP-HV, VV, HH_VV.

The classification improvement using the coherence information with intensity images was noticed for all multi-band sets except for SS-HH, HV whose overall accuracy is higher than the SS-HH, VV, H1_HH2 result.

Table 1 - Results of SegSAR (SS) and SPRING (SP) classifications.

# Channel	Channels	Overall Accuracy (%)		$\hat{\kappa}$		$\sigma^2_{\hat{\kappa}}$ (x10^{-5})	
		SS	SP	SS	SP	SS	SP
3	HV, VV, HV1_HV2	97.97	76.85	0.9738	0.7079	2.15	18.72
3	HH, HV, HH_VV	94.23	79.34	0.9253	0.7331	5.79	15.37
3	HH, VV, HV1_HV2	94.16	60.79	0.9254	0.5106	6.02	28.54
3	HH, HV,HV1_HV2	87,80	55.28	0.8469	0.4533	11.26	28.72
3	HV,VV, HH1_HH2	86.29	81.18	0.8284	0.7645	12.81	16.37
3	HH, HV, HH1_HH2	83.28	85.31	0.7856	0.8154	15.44	11.55
3	HV, VV, HH_VV	80.90	87.61	0.7641	0.8445	15.57	11.42
3	HH, VV, HH_VV	80.59	79.41	0.7541	0.7407	17.25	15.32
3	HH, VV, HH1_HH2	77.84	86.30	0.7260	0.8257	17.67	12.87
2	HH, HV	80.07	77.18	0.7512	0.7138	16.14	17.60
2	HV, VV	72.20	72.00	0.6545	0.6445	19.14	19.10
2	HH,VV	57.38	61.84	0.4863	0.5221	25.35	25.55

4. REFERENCES

[1] L. A. Silva, G.B. Scofield, S. R. Aboud Neta, R. G. Negri, L. V. Dutra, and C. C. Freitas, "Utilização de imagens de coerência interferométrica em banda L para classificação de cobertura da terra na região de Tapajós-PA." In: ***Simpósio Brasileiro de Sensoriamento Remoto***, 14. (SBSR), 2009, Natal. Proceedings. São José dos Campos: INPE, 2009. p. 7489-7496

[2] G. B. Scofield; L. V. Dutra, D. L. A. Silva, R. G. Negri, S. R. Aboud Neta, and C. C Freitas, "Mapeamento da cobertura da terra na Floresta Nacional de Tapajós - PA utilizando imagem de coerência polarimétrica." In: ***Simpósio Brasileiro de Sensoriamento Remoto***, 14. (SBSR), 2009, Natal. Proceddings. São José dos Campos: INPE, 2009. p. 6227-6232.

[3] Sousa Júnior, M. A. *Segmentação multi-níveis e multi-modelos para imagens de radar e ópticas.* 2005. 131 p. (INPE-14466-TDI/1147). PhD Thesis (in portuguese) - Instituto Nacional de Pesquisas Espaciais, São José dos Campos. 2005.

[5] G. Camara, R.C.M Souza. , U.M. Freitas, J. Garrido *SPRING: Integrating remote sensing and GIS by object-oriented data modeling*. Computers & Graphics, vol. 20, n.3, pp.395-403, 1996.

[5] Henderson F. M., and A. J Lewis. ***Manual of remote sensing: principles and applications of imaging radar***, 3rd edition, John Wiley Sons, USA, v. 2, 896p, 1998.